

Benzocyclobutene (BCB) Based Neural Implants with Microfluidic Channel

K. Lee¹, J. He¹, L. Wang²

¹Arizona Biodesign Institute and Harrington Department of Bioengineering, Arizona State University, Tempe, AZ, USA

²Department of Chemical Engineering, Arizona State University, Tempe, AZ, USA
jjiping.he@asu.edu

Abstract—Benzocyclobutene (BCB) based intracortical neural implants for basic neuroscience research in animal models was fabricated, in which microfluidic channel was embedded to deliver chemical reagents. BCB presents several attractive features for chronic applications: flexibility, biocompatibility, desirable chemical and electrical properties, and can be easily manufactured using existing batch microfabrication technology. The fabricated implants have single shank with three recording sites (20 x 20 μ m) and two reservoirs (inlet and outlet). The channel had large volume (40 μ m width and 10 μ m height), and hydrophobic surface to provide a high degree of chemical inertness. All the recording sites were positioned near the end of the shank in order to increase the probability of recording neural signals from a target volume of tissue. In vitro biocompatibility tests of fabricated implants revealed no adverse toxic effects on cultured cells. The implant with a 5 μ m silicon backbone layer penetrated rat's pia without buckling, a major drawback of polymer alone. The averaged impedance value at 1KHz was ~1.2 MW. Water flowing through the channel was observed. Depending on the amount of the driving pressure from the syringes, the delivery speed of the water was totally controlled.

Keywords—Benzocyclobutene (BCB), bioMEMS, electrodes, microfluidic channel, neural implant, polymer

I. INTRODUCTION

Recently, we reported the fabrication of polyimide based multichannel intracortical neural implants and recorded the neural activities from the auditory cortex of a rat's brain [1, 2]. This type of polymer material presents several attractive features for chronic applications: flexibility, biocompatibility, desirable chemical and electrical properties, and can be easily manufactured using existing batch microfabrication technology. The flexibility is highly desirable to minimize tissue damage at the brain-tissue/implant interface. Unfortunately, there are two key issues associated with the flexible polyimide electrodes. Due to the lack of stiffness, polymer electrodes easily buckle during insertion and therefore, cannot penetrate the pia during surgery. Second, the polyimide has relatively high moisture uptake (~4wt%), which leads to a rapid fall in electrode impedance, ultimately leading to electrode failure.

Here we report a new type of polymer-based neural implant using benzocyclobutene (BCB) as the substrate. BCB's unique properties of extremely low moisture uptake 0.12 wt% and low dielectric constant of 2.64 suggest that this class of polymer will outperform polyimide for chronic implant application. For easy handling of the electrode during surgical insertion into neural tissues, a 5 μ m thick

silicon backbone layer, from silicon-on-insulator (SOI) substrate, was attached to the desired region of the electrode to increase the stiffness. Wafer thickness (~200 μ m) was remained in the connector portion of the electrode to facilitate the electrode handling and fit to 15-channel commercial connector spacing.

BCB based intracortical neural implant was fabricated, in which microfluidic channel was embedded to deliver some solutions such as stimulus of the neural reaction in brain. Fig. 1 shows schematic diagram of the fabricated electrode. The channel was located in the middle of the silicon backbone layer, and had hydrophobic surface to provide a high degree of chemical inertness. This paper describes the design, fabrication, and initial testing results of the latest prototype BCB-based intracortical implant with micro-fluidic channel.

II. FABRICATION OF NEURAL IMPLANT

We started fabrication with a 4-in SOI substrate with 5 μ m thick top device silicon and 1 μ m thick buried silicon dioxide. Top device silicon was (100) oriented n-type silicon with resistivity of 10~25 Ohm-cm. Fig. 2 shows schematic diagrams for the fabrication procedure. First, approximately 3 μ m thick top device silicon was etched away in reactive ion etch (RIE) for 2 minutes with SF₆ (Fig. 2(a)) using a photoresist (PR) masking layer. After dissolving PR masking layer, a 10 μ m thick sacrificial layer of AZ 4620 PR was spun and defined for the microfluidic channel (Fig. 2(b)). This layer determines the cross-sectional area of the drug delivery microchannel (structural dimension).

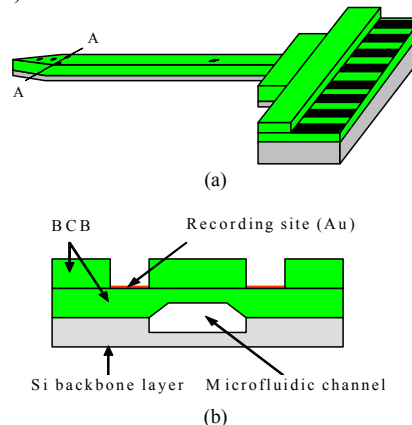


Fig. 1. Simple schematic diagram of the BCB based neural implant with microfluidic channel: (a) Top view and (b) cross-sectional view of A-A.

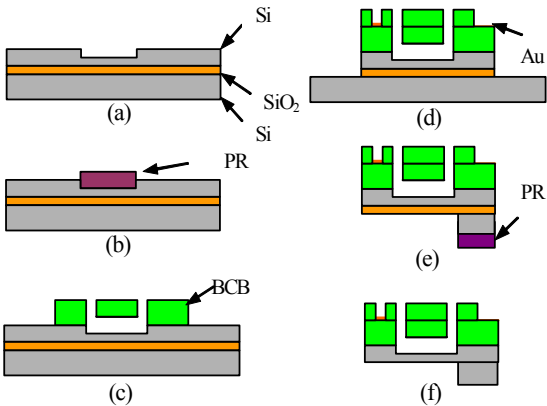


Fig. 2. Fabrication procedure of the BCB electrode with microfluidic channel. (a) top device silicon dry-etching using a photoresist masking layer, (b) sacrificial layer pattern for microfluidic channel, (c) the base layer of BCB, (d) the upper layer of BCB, (e) selective backside silicon etching with masking layer, and (f) buried SiO₂ etching and final electrode.

Next a 2 μm thick parylene-C layer was deposited to seal the sacrificial layer. Here the parylene-C layer prevents the BCB solvents from attacking the soft sacrificial resist. The first layer of photosensitive BCB was spin-coated, exposed, and then developed to encapsulate or reveal the desired regions. BCB layer was dried in air for 2 days. The opening holes were not completely opened, probably due to a lateral penetration of ultraviolet (UV) light. RIE was used to etch away the BCB residue on the opening surface using a 10 μm thick photoresist-masking layer. A CF₄ and O₂ mixture was used for RIE (100Watt, 100mTorr, 10sccm CF₄, and 40sccm O₂). Then the parylene-C layer was dry-etched in RIE down to the sacrificial layer. Access holes to the sacrificial layer were patterned. The protective resist and the sacrificial layer were next dissolved in acetone for 3 hours (Fig. 2(c)). BCB layer was not damaged by acetone. After rinsing the device in isopropyl alcohol and DI water, the BCB layer was partially cured for 30 minutes at 200°C in N₂ gas environment to protect the developed pattern from subsequent processing steps.

A reactive ion etch (RIE) was used to clean and micro-roughen the BCB surface. After RIE, a 2000Å thick gold layer was deposited for recording sites, followed by wet etching. Gold was used for recording sites because it has excellent surface inertness, and it provides no native oxide. The top BCB layer was spun, exposed, and developed to encapsulate or reveal the desired regions (Fig. 2(d)). The electrode was then fully cured for 1 hour at 210°C in N₂ gas environment. RIE was used to etch away the BCB residue over the surface. The final BCB structures are approximately 20 μm thick. Partial cure of the base BCB layer and full cures of the upper BCB layer terminated any route for water transmission through the boundary between the base and top BCB layers. Compared to polyimide electrode (~30% volume shrinkage during full cure), BCB

had less shrinkage during the curing process (~5% shrinkage).

The wafer was flipped over and patterned with a photoresist for selective backside silicon etching in DRIE. Masked portion of silicon was not etched from dry etching in DRIE. The top device surface was protected from plasma heat and RF power on the ground plane with photoresist and another dummy silicon wafer. Backside silicon etching was performed for 3hrs in DRIE. A clean and uniform silicon backside etching was obtained. Silicon etching exactly stopped on the buried SiO₂ layer due to big etching rate difference between Si and SiO₂ (Fig. 2(e)). After complete removal of backside silicon, the buried SiO₂ was etched away in 49% HF acid solution (Fig. 2(f)) for 30 seconds. Finally top-protecting photoresist and bottom masking layer was dissolved in microstripe for 2hr at 50°C. Several rinses with de-ionized water are performed to remove any unwanted etchant products.

III. RESULTS

A. Fabricated Devices

The fabricated devices were visualized through optical microscopy and scanning electron microscopy (SEM), as shown in Fig. 3. The fabricated implant had one shank with 3 recording sites (20 \times 20 μm) and 2 reservoirs (inlet and outlet). The total length of the completed electrode was 11mm, and the thickness of the electrode tip portion was approximately 25 μm . The thickness of the connector portion was ~200 μm . The wafer thickness of the connector portion gave easy handling during insertion into the 15-channel connector. The channel had large volume (40 μm width and 10 μm height), and hydrophobic surface to provide a high degree of chemical inertness. The inlet opening was 40 \times 100 μm , and the outlet opening was 40 \times 40 μm . All the recording sites were positioned near the end of the shank in order to increase the probability of recording neural signals from a target volume of tissue.

B. Biocompatibility Test

Before insertion into brain, the fabricated electrode should meet a strict biocompatibility standard. Our electrodes are composed of BCB, gold, silicon, and parylene-C. The cell adhesion behavior of a completed electrode exposed to monolayers of 3T3 fibroblasts (ATCC #CRL-6476) cell line in vitro was studied using a Live/Dead Viability/Cytotoxicity Kit (L-3224, Molecular Probes) and previously described methods [3]. The morphology of 3T3 cells showed conformal coverage over all the surfaces and was similar to cells cultured on tissue culture plastic (Fig. 4 (a, b)). Thus the completed electrode was considered a non-toxic substrate for cell adhesion and cell growth.

Next we modified the BCB surface with ammonia plasma treatment to improve biocompatibility. BCB surface

will contact with blood or protein in brain. Amine functional groups, which are attached by ammonia plasma treatment, will provide a stable hydrophilic BCB surface and protein repelling surface. Fig. 4(c) shows 3T3 cell adhesion and spreading on ammonia plasma-treated BCB surface. Cell adhesion was significantly reduced, because the covalent coupling of oxidized dextran to modified surface repels the cell adhesion and spreading.

C. Electrical Impedance Test

Electrical impedance measurement was performed in saline to characterize recording sites of the BCB electrode and electrolyte interface.

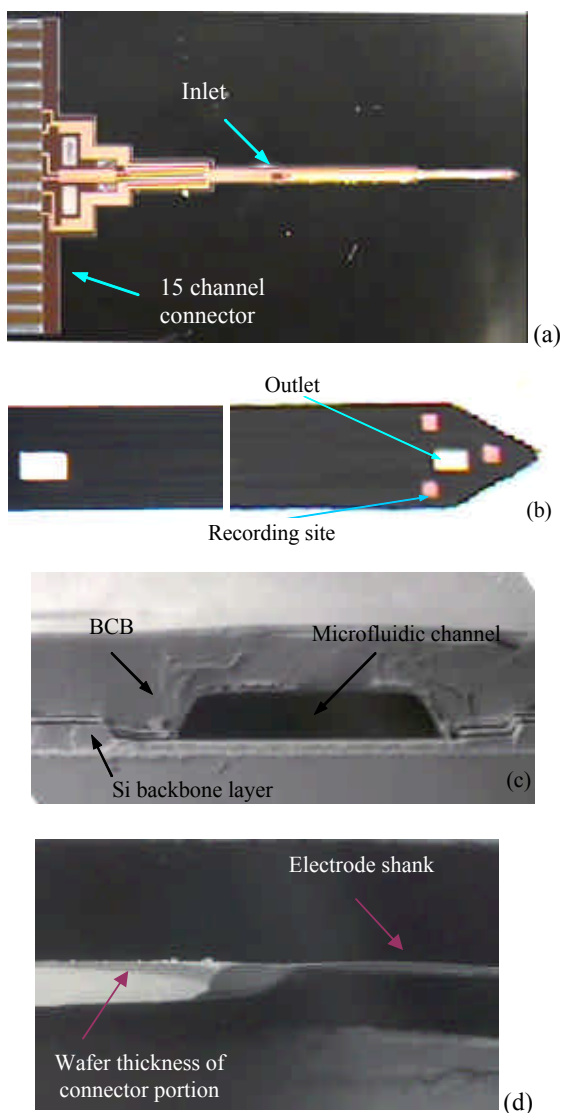


Fig. 3. Optical microscope and SEM images of the fabricated electrode. (a) Entire view of the electrode, (b) top view of the single shank, (c) microfluidic channel, and (d) cross-sectional view of connector portion.

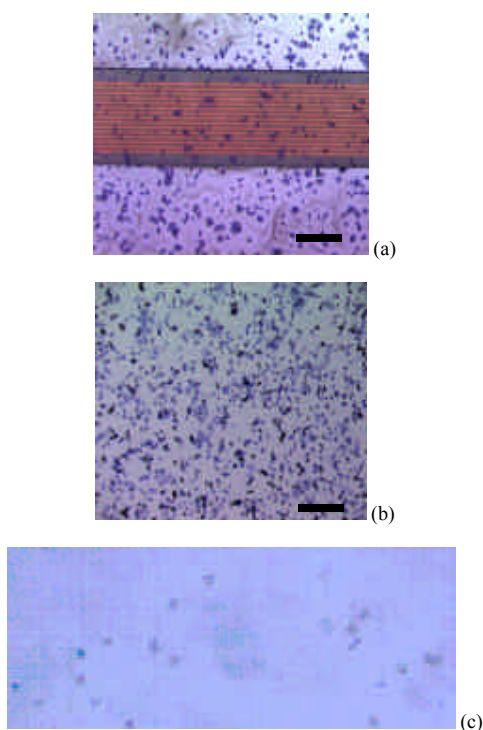


Fig. 4. Photomicrographs depicting morphology of adherent 3T3 cells on BCB electrode. (a) Image of cells adherent to electrode shank and surrounding wafer surface; Scale Bar = 100 μm . (b) Image of cells adherent to tissue culture plastic; Scale Bar = 100 μm . (c) Cell adhesion and spreading on ammonia plasma-treated BCB surface.

Measurement was performed using HP 4284A precision LCR meter. The shafts were immersed into a 0.9% saline solution at room temperature. A platinum wire was used as the reference electrode. Three devices (3 recording sites per device) were tested and the area of the recording site was $20 \times 20 \mu\text{m}$. The frequency was varied from 100 Hz to 10 KHz, while the alternating peak-to-peak current source was set at $100 \mu\text{A}$. Fig. 5 shows the averaged impedance values from three recording channels. The averaged impedance values at 1 KHz were $\sim 1.2 \text{ Mohm}$. We believe the observed impedance data is acceptable for recording. The phase angle θ was negative and remained near -25 degree at 1 KHz. When the phase angle $\theta < -80$ it becomes capacitive which is undesirable for recording purpose. Impedance remained stable over 48 hours because of extremely low moisture uptake in the BCB dielectric layers. The observed averaged impedance value of 1.2 Mohm at 1 KHz is comparable with the reported values for similar electrodes [4, 5]. In vivo and long-term impedance stability characterizations are the focus of further investigation.

D. Mechanical Test

Pure polymer BCB electrode without silicon backbone layer is flexible, and thus it can be bended more than 90

degrees without any damages of the film. By adding a $5\mu\text{m}$ thick silicon backbone layer, the flexibility diminishes. To determine whether BCB substrate and gold metal traces are stable after ~ 90 degree bending, we intentionally applied 90 degree bending force to the electrode. Any visual damage of the BCB film was not observed in the SEM picture, but silicon layers were fractured.

Penetration test into rat's brain was performed to check whether the microprobe could penetrate the pia and dura without any surgery aid tool. Rat was anaesthetized and heart rate and oxygen saturation were monitored. Skull and dura were removed and the stiff electrode was lowered to the surface (pia) by hand. Enough force was applied using Teflon tweezer. Stiff electrodes with $5\mu\text{m}$ thick backbone silicon penetrated pia of rat without buckling (Fig. 6).

E. Delivery Test

To verify that the channel is entirely opened, we tested two things: First, the center of the microfluidic channel was cleaved by a diamond cutter and then took SEM pictures. Before cutting, the samples were immersed in liquid N_2 gas to prevent any damage in BCB layer during cutting. Clearly opened channel was obtained as shown in Fig. 3(c). The photoresist residues over the channel wall surface were not observed due to low temperature PR soft baking before removing the sacrificial layer.

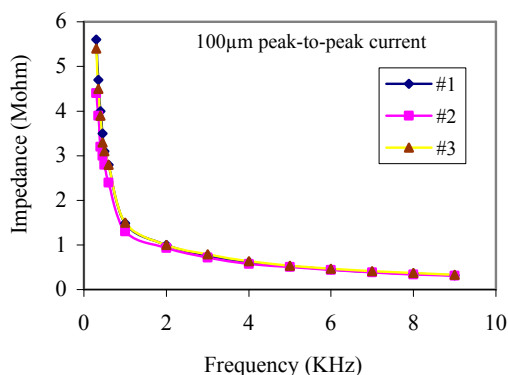


Fig. 5. Averaged impedance values from 3 devices after 48-hour immersion. The recording site is $20 \times 20\mu\text{m}$ and electrode is gold.

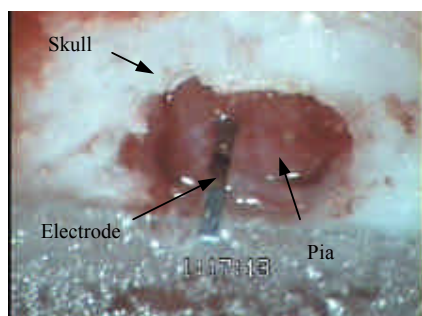


Fig. 6. Optical microscope picture of the penetration test into rat's pia. A $5\mu\text{m}$ silicon backbone BCB electrode is penetrating pia without buckling.

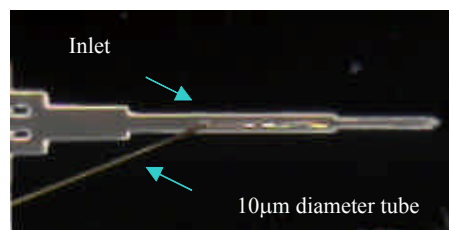


Fig. 7. Optical microscope picture of water delivery test. A $10\mu\text{m}$ diameter tube was inserted into the inlet opening while the other opening (outlet) was left open.

Second, the flow characteristics of the channel were tested. A $10\mu\text{m}$ diameter tube connected to a syringe was inserted into the inlet opening (Fig. 7) and then tightly bonded using epoxy while the other opening (outlet) was left open. From the syringe, water was pressured down, and at the outlet opening, water appearance was observed. The syringe provides the flow driving force. Water flowing through the channel was observed. Depending on the amount of the driving pressure from the syringes, the delivery speed of the water was totally controlled.

IV. CONCLUSION

We have presented a complete fabrication process of polymer-based multichannel intracortical neural implant with microfluidic channel. In vitro biocompatibility tests of prototype implants, the completed BCB electrode has no adverse toxic effect on cell adhesion and cell growth. Stiff BCB electrodes with $5\mu\text{m}$ thick backbone silicon penetrated pia of rat without buckling, a major drawback with polymer material. The averaged impedance value at 1KHz was $\sim 1.2\text{ M}\Omega$. Depending on the amount of the driving pressure from the syringes, the delivery speed of the water through microfluidic channel was totally controlled.

REFERENCES

- [1] P. Rousche, D. Pellinen, D. Pivin, J. Williams, R. Vetter, and D. Kipke, "Flexible polyimide-based intracortical electrode arrays with bioactive capability," *IEEE Trans. Biomedical Eng.*, vol. 48, no. 3, pp. 361-371, 2001.
- [2] K. Lee, A. Singh, H. Zhu, G. Coryell, B. Olson, B. Kim, G. Raupp, and J. He, "Fabrication of implantable polyimide based neural implants with flexible regions to accommodate micromovement," in *Proc. 12th International Conf. Solid-State Sensors, Actuators, and Microsystems (Transducers '03)*, Boston, MA, pp. 1221-1224.
- [3] J. Trudel and S. Massia, "Assessment of the cytotoxicity of photocrosslinked dextran and hyaluronan-based hydrogels to vascular smooth muscle cells," *Biomaterials*, vol. 23, pp. 3299-3397, 2002.
- [4] N. Blum, B. Carkhuff, H. Charles, R. Edwards, and R. Meyer, "Multisite microprobes for neural recordings," *IEEE Trans. Biomedical Eng.*, vol. 38, pp. 68, 1991.
- [5] T. Yoon, E. Hwang, D. Shin, S. Park, S. Oh, S. Jung, H. Shin, and S. Kim, "A micromachined silicon depth probe for multichannel neural recording," *IEEE Trans. Biomedical Eng.*, vol. 47, pp. 1082, 2000.